GSA DATA REPOSITORY 2014351

Supplementary Material for
"Enhanced carbon dioxide outgassing from the eastern equatorial Atlantic during the last glacial"
by Foster and Sexton

Sample Material and sampling locations

Fig. 1 shows the location of the sites used in this study. The average sedimentation rates for the sites are relatively high at 4.9 cm/kyr (GeoB1105-4; hereafter GeoB1105), 2.6 cm/kyr (GeoB1523-1, hereafter GeoB1523) and 4.7 cm/kyr (ODP 999). Age models for the studied period are discussed in Henehan et al. (2013) for ODP 999 and GeoB1523, and based on C-14 dating for GeoB1105-4 (Bickert and Mackensen, 2003).

In order to reconstruct the mixed layer carbonate system the foraminiferal species *G. ruber* (white; sensu stricto) from the 300-355 μm size fraction is used here. Sediment trap data from the equatorial Atlantic and Caribbean suggest that this species from all three sites will record environmental signals biased towards the spring, summer and autumn rather than annual average (Tedesco and Thunell, 2003; Frail et al., 2008 and references therein).

The location of boreal summer equatorial upwelling, with respect to sites GeoB1105, GeoB1523 and ODP 999, is visible on a map of annual SST and mean annual biological productivity (Figure 1a & b). The magnitude of the CO_2 flux evident for this region in the climatology of Takahashi et al. (2009; Fig. 1d) is rather small (25 to 30 μatm). However, several studies document upwelling in the eastern equatorial Atlantic near site GeoB1105 are periodically characterised by ΔpCO_2 of up to 80-100 ppm (Bakker et al., 2001).

Analytical Methodology

For boron isotope and trace metal analysis foraminifera were cleaned using standard trace element cleaning techniques involving oxidation with buffered 1% H_2O_2 (Barker et al., 2003) and between 100 and 120 tests of *G. ruber* (300-355 μm ~1-2 mg of $CaCO_3$ = 20-30 ng of B) were dissolved in 0.5 M HNO_3. Boron isotope composition of chemically purified B was carried out on a Thermo Scientific Neptune MC-ICPMS at the University of Bristol (see Foster (2008) for details). Analytical uncertainty, as discussed in Foster (2008), is ± 0.25 ‰ (at 95% confidence) based on the reproducibility of in-house carbonate standards.

Mg/Ca ratios were determined on a small aliquot (~5 %) of the solution used for isotope analysis using a Thermo Scientific Element 2 at the University of Bristol (following Foster, 2008). Based on repeat measurements of our consistency standard over the duration of this study we calculate an uncertainty on Mg/Ca to be ± 3 % (95 % confidence).

The boron isotope proxy and estimates of pH and pCO_2^{sw}

The basis for the boron isotope–pH proxy is discussed extensively elsewhere (e.g. Henehan et al., 2013; Rae et al., 2011; Foster 2008; Hönisch and Hemming, 2005). For the planktic foraminifer species *G. ruber* used here, following Henehan et al. (2013), vital effects relating to the activity of photosymbionts can be corrected by the following equation:

$$\delta^{11}B_{borate} = (\delta^{11}B_{G.\ Ruber} - 8.87)/0.6 \quad (1)$$

the following equation can then be used to calculate pH values from the calculated $\delta^{11}B$ of borate (following Henehan et al., 2013):

$$pH = pK_B^* - \log\left(-\frac{\delta^{11}B_{B_T} - \delta^{11}B_{B(OH)_4^-}}{\delta^{11}B_{B_T} - 1.0272 \cdot \delta^{11}B_{B(OH)_4^-} - 27.2}\right) \quad (2)$$

where pK_B^* is the pK^* value for boric acid at the in situ temperature and salinity (Dickson, 1990), $\delta^{11}B_T$ is the isotopic composition of seawater ($\delta^{11}B$ = 39.61 ‰; Foster et al., 2010), $\delta^{11}B_{B(OH)4-}$ is the measured isotopic composition of borate ion determined from the $\delta^{11}B$ of *G. ruber*, and 27.2 and 1.0272 ‰ is the isotopic fractionation between borate ion and boric acid (Klochko et al., 2006).

Estimates of sea surface temperature (SST) and sea surface salinity (SSS) are required in order to calculate pH from $\delta^{11}B$, due to the influence of these parameters on pK_B^*. For sites GeoB1105 and GeoB1523 SST is reconstructed using the Mg/Ca ratio of *G. ruber* measured on an aliquot of the same sample used for isotope measurement and the generic SST equation of Anand et al. (2003); which gives best agreement with annual mean SST at each site; Figure 2a):

$$Mg/Ca = 0.38 * EXP(SST*0.09) \quad (3)$$

For site 999 the Mg/Ca data of Schmidt et al. (2004) is interpolated and used with an offset of +0.66 mmol/mol to account for an interlaboratory and technique bias (Schmidt et al., 2004 used a full reductive clean known to lower Mg/Ca by ~10%; Hertzberg and Schmidt, 2013). The magnitude of this bias was determined through a comparison of Mg/Ca measured at Bristol at lower resolution on *G. ruber* from the same site over the last 130 kyr. To reflect uncertainty in the potential, but debated (Arbuszewski et al. 2010; Hönisch et al., 2013; Hertzberg and Schmidt 2013), influence of salinity on Mg/Ca-based SST's, and accounting for our analytical uncertainty, we use an uncertainty in SST of ± 1.5 ^oC (at 95% confidence).

Salinity has only a minor influence on the pCO_2^{sw} calculated using the boron isotope technique (1.8 µatm per psu) and here we chose to keep it at modern values for each location and propagate a generous level of uncertainty (± 3 psu).

Given an estimate of total alkalinity (we assume a constant value of 2300 µmol/kg which is close to the modern value at each location) and a $\delta^{11}B$-derived pH it is possible to reconstruct the entire carbonate system including $[CO_2]_{aq}$ and hence pCO_2^{sw} (see Foster (2008) for details). In order to fully propagate the various

uncertainties relating to each reconstruction we use a Monte Carlo approach (n=10,000) and the following uncertainties (at 95% confidence): ±3 psu, ±1.5 ^{o}C, ± 150 μmol/kg total alkalinity, ± δ^{11}B analytical uncertainty (±0.25 ‰). It is important to note that despite these being conservative estimates of the uncertainty associated with these parameters the typical uncertainty in the reconstructed pH is ± 0.03 pH units and ± 30 μatm for pCO_2^{sw} (note the uncertainties are however not exactly symmetrical). An alternative method to reconstruct total alkalinity (TA), based on the modern total alkalinity to salinity relationship in the equatorial Atlantic (TA = Salinity x 61.88+162.66, Key et al., 2004) and reconstructions of salinity based on sea-level (salinity = $\text{salinity}_{\text{modern}} + \Delta_{\text{sea-level}} / 3800 * 34.8$; see Hönisch and Hemming, 2005) are well within the Monte Carlo uncertainty band (dotted lines on Fig 2d), illustrating that our assumptions regarding the second carbonate system parameter do not unduly impact our pCO_2^{sw} reconstructions.

All carbonate chemistry calculations were undertaken here using the equations and constants recommended and outlined in Dickson et al. (2007) and using the R-package seacarb (see http://cran.r-project.org/web/packages/seacarb/index.html). The total pH scale is used throughout. All analytical data and calculated carbonate system parameters are tabulated in Table DR1.

Estimates of surface water [PO_4^{3-}] and the rate of glacial-aged upwelling in the Eastern Atlantic

In order to estimate surface water [PO_4^{3-}] over the last 30 kyr at GeoB1105 we used two independent methods: (i) given a record of atmospheric CO_2, and the modern degree of air:sea disequilibrium with respect to CO_2, it is possible to calculate the excess of dissolved inorganic carbon given the observed ΔpCO_2 at site GeoB1105. This excess is 60-80 μM during the last glacial period (average 71 μM for the period 18 to 25 kyr). By assuming modern Redfield Ratios (C:N:P = 106:16:1), this excess-DIC is associated with 71/106 μM = 0.67 μM [PO_4^{3-}]. Figure DR1 shows a time series of [PO_4^{3-}] calculated in this manner. (ii) We have also used the observed west to east δ^{13}C gradient in *G. ruber* from ODP 999 and GeoB1105 over the last 30 kyr (Schmidt et al., 2004; Mulitza et al., 1998), assumed [PO_4^{3-}] remains close to zero in the Caribbean throughout the last 30 kyr , which enables us to convert the E-W δ^{13}C gradient into [PO_4^{3-}] using the modern relationship between these terms (1‰ increase in δ^{13}C = 1.1 μM decrease in [PO_4^{3-}]; Broecker and Maier-Reimer, 1992). Despite the simplicity of this approach (i.e. we are neglecting the influence of out-gassing and $\Delta CO_3^{=}$ on δ^{13}C; Broecker and Maier-Reimer, 1992; Spero et al., 1997), this approach gives a remarkably close secular evolution (Figure DR1) and a very similar average (0.76 μM [PO_4^{3-}]) for the interval 18 to 25 kyr to the boron isotope based estimate .

As discussed in Sigman and Haug (2003), at steady state Broecker and Peng (1982) described the following expression to indicate the balance between gross upward (left-hand side) and gross downward (right-hand site) of phosphorous (which can proxy for all macro-nutrients) in the surface ocean:

$$[\mathrm{PO_4^{3-}}]_{\mathrm{deep}} \times Q = [\mathrm{PO_4^{3-}}]_{\mathrm{surface}} \times Q + EP_p$$

where $[PO_4^{3-}]$ is the phosphate concentration in the deep and surface water layers, EP_p is the export production in terms of phosphorous and Q is the exchange rate of water between the deep and the surface (i.e. upwelling rate):

$$Q = \frac{EP_p}{\left([PO_4^{3-}]_{deep} - [PO_4^{3-}]_{surface}\right)} = 0.74$$

The reconstruction of Schmidt et al. (2003) indicates an approximate three-fold increase in primary production. For simplicity we assume that *EPp* scales linearly with primary production for the last glacial period (Fig. 3). If we assume modern subsurface values of $[PO_4^{3-}]$, glacial-aged Q (upwelling rate) is 3.75 (an increase by a factor of 5). It has recently been suggested on the basis of $\delta^{15}N$ data from the Caribbean that during the last glacial maximum the nutrient content of water upwelling in the eastern equatorial Atlantic was lower than today (because of the replacement of comparatively nutrient-rich AAIW with nutrient-depleted GNAIW; Straub et al., 2013). Any reduction in $[PO_4^{3-}]_{deep}$ will only serve to increase our estimates of Q and vice versa. For example a $[PO_4^{3-}]_{deep}$ of 1 µM increases Q to 10, a 14x increase in upwelling rate.

Reference List (for supplementary material)

Anand, P., Elderfield, H., and Conte, M., 2003, Calibration of Mg/Ca thermometry in planktonic foraminifera from a sediment trap time series: Paleoceanography, v. 18, p. 1050, doi:10.1029/2002PA000846.

Arbruszewski, J., deMonocal, P.B., Kaplan, A., and Farmer, E.C., 2010, On the fidelity of shell-derived $\delta^{18}O_{seawater}$ estimates: Earth and Planetary Science Letters, v. 300, p. 185-196.

Bakker, D.C.E., Etcheto, J., Boutin, J., and Merlivat, L., 2001, Variability of surface water fCO_2 during seasonal upwelling in the equatorial Atlantic Ocean as observed by a drifting buoy: Journal of Geophysical Research, v. 106, p. 9241-9253.

Barker, S., Greaves, M., and Elderfield, H., 2003, A study of cleaning procedures used for foraminiferal Mg/Ca paleothermometry: Geochemistry, Geophysics, Geosystems, v. 4, p. 8407, dio:10,1029/2003GC000559.

Bickert, T., and Mackensen, A., 2003, Last glacial to Holocene changes in South Atlantic Deep Water circulation, *in* Wefer, G., Mulitza, S., and Ratmeyer, V., eds., The South Atlantic in the Late Quaternary: Reconstruction of material budgets and current systems: Berlin Heidelberg, Springer-Verlag, p. 671-695.

Broecker, W.S., and Peng, T., -H., 1982, Tracers in the Sea, Eldigio Press, Palisades, New York.

Broecker, W.S., and Maier-Reimer, E., 1992, The influence of air and sea exchange on the carbon isotope distribution in the sea: Global Biogeochemical Cycles, 6, 315-320.

Dickson, A., Sabine, C., and Christian, J., 2007, Guide to best practises for ocean CO_2 measurements.: Sidney, British Columbia, North Pacific Marine Science Organization.

Dickson, A.G., 1990, Thermodynamics of the dissociation of boric acid in synthetic seawater from 273.15 to 318.15 K: Deep Sea Research Part A. Oceanographic Research Papers, v. 37, p. 755-766.

Foster, G.L., 2008, Seawater pH, pCO_2 and $[CO_3^{2-}]$ variations in the Caribbean Sea over the last 130 kyr: A boron isotope and B/Ca study of planktic foraminifera: Earth and Planetary Science Letters, v. 271, p. 254-266.

Foster, G.L., Pogge von Strandmann, P.A.E., and Rae, J.W.B., 2010, Boron and magnesium isotopic composition of seawater: Geochemistry Geophysics Geosystems, v. 11, p. Q08015, doi:10.1029/2010GC003201.

Fraile, I., Schulz, M., Mulitza, S., and Kurcera, M., 2008, Predicting the global distribution of planktonic foraminifera using a dynamic ecosystem model: Biogeosciences, v. 5, p. 891-911.

Henehan, M.J., Rae, J.W.B., Foster, G.L., Erez, J., Prentice, K.C., Kurcera, M., Bostock, H.C., Martinez-Boti, M.A., Milton, J.A., Wilson, P.A., Marshall, B., and Elliott, T., 2013, Calibration of the boron isotope proxy in the planktonic foraminifera *Globigerinoides ruber* for use in palaeo-CO_2 reconstruction: Earth and Planetary Science Letters, v. 364, p. 111-122.

Hertzberg, J.E., and Schmidt, M.W., 2013, Refining *Glogerinoides ruber* Mg/Ca paleothermometry in the Atlantic Ocean: Earth and Planetary Science Letters, v. 383, p. 123-133.

Hönisch, B., Allen, K.A., Lea, D., Spero, H.J., Eggins, S.M., Arbuszewski, J., deMonocal, P.B., Rosenthal, Y., Russell, A.D., and Elderfield, H., 2013, The influence of salinity on Mg/Ca in planktic foraminifers - Evidence from cultures, core-top sediments and complementary $\delta^{18}O$: Geochmica et Cosmochimca Acta, v. 121, p. 196-213.

Hönisch, B., and Hemming, N.G., 2005, Surface ocean pH response to variations in pCO_2 through two full glacial cycles: Earth and Planetary Science Letters, v. 236, p. 305-314.

Key, R.M., Kozyr, A., Sabine, C.L., Lee, K., Wanninkhof, R., Bullister, J.L., Feely, R.A., Millero, F.J., Mordy, C., and Peng, T.-H., 2004, A global ocean carbon climatology: Results from Global Data Analysis Project (GLODAP): Global Biogeochemical Cycles, v. 18, p. GB4031, doi:10.1029/2004GB002247.

Klochko, K., Kaufman, A.J., Yoa, W., Byrne, R.H., and Tossell, J.A., 2006, Experimental measurement of boron isotope fractionation in seawater: Earth and Planetary Science Letters, v. 248, p. 261-270.

Mulitza, S., Rühlemann, C., Bickert, T., Hale, W., Pätzold, J., and Wefer, G., 1998, Late Quaternary $\delta^{13}C$ gradients and carbonate accumulation in the western equatorial Atlantic: Earth and Planetary Science Letters, v. 155, p. 237-249.

Rae, J.W.B., Foster, G.L., Schmidt, D.N., and Elliott, T., 2011, Boron isotopes and B/Ca in benthic foraminifera: proxies for the deep ocean carbonate system: Earth and Planetary Science Letters, v. 302, p. 403-413.

Schmidt, D.N., Renaud, S., and Bollmann, J., 2003, Response of planktic foraminiferal size to late Quaternary climate change: Paleoceanography, v. 18, p. 1039, doi:10.1029/2002PA000831.

Schmidt, M.W., Spero, H.J., and Lea, D.W., 2004, Links between salinity variation in the Caribbean and North Atlantic thermohaline circulation: Nature, v. 428, p. 160-163.

Sigman, D.M., and Haug, G.H., 2003, The biological pump in the past, *in* Elderfield, E, eds, The Oceans and Marine Geochemistry, Vol. 6 *Treatise on Geochemistry*, Elsevier-Pergamon, Oxford, p. 491-528.

Spero, H.J., Bijma, J. Lea, D.W., Bemis, B.E., 1997, Effect of seawater carbonate concentration on foraminiferal carbon and oxygen isotopes: Nature, 390, 497-500.

Straub, M., Sigman, D.M., Ren, H., Martinez-Garcia, A., Meckler, A.N., Hain, M.P., and Haug, G.H., 2013, Changes in North Atlantic nitrogen fixation controlled by ocean circulation: Nature, v. 501, p. 200-203.

Takahashi, K., Sutherland, S.C., Wanninkhof, R., Sweeney, C., Feely, R.A., Chipman, D.W., Hales, B., Friederich, G., Chavez, F., Sabine, C., Watson, A., Bakker, D.C.E., Schuster, U., Metzl, N., Yoshikawa-Inoue, H., Ishii, M., Midorikawa, T., Nojiri, Y., Kortzinger, A., Steinhoff, T., Hoppema, M., Olafsson, J., Arnarson, T.S., Tilbrook, B., Johannessen, T., Olsen, A., Bellerby, R., Wong, C.S., Delille, B., Bates, N.R., and de Baar, H.J.W., 2009, Climatological mean and decadal change in surface ocean pCO_2, and net sea-air CO_2 flux over the global oceans: Deep-Sea Research II, v. 56, p. 554-577.

Tedesco, K.A., and Thunell, R.C., 2003, Seasonal and interannual variations in planktonic foraminiferal flux and assemblage composition in the Cariaco Basin, Venezuela: Journal of Foraminiferal Research, v. 33, p. 192-210.

Table DR1. Summary of boron isotope and Mg/Ca data

Site	Depth (m)	Age (kyr)	$d^{11}B$	$d^{11}B$ 2s	Mg/Ca	SST (^{o}C)	pCO_2^{sw} (µatm)	pCO_2^{sw} 2.5%	pCO_2^{sw} 14 %	pCO_2^{sw} 86%	pCO_2^{sw} 97.5%
GeoB1105-4	0.36	9.2	20.34	0.25	3.81	25.6	300	273	285	319	331
GeoB1105-4	0.46	11.4	20.65	0.25	4.03	26.2	270	251	256	285	290
GeoB1105-4	0.55	13.3	20.58	0.25	3.77	25.5	277	257	262	289	300
GeoB1105-4	0.65	14.6	20.72	0.25	3.54	24.8	256	229	244	273	278
GeoB1105-4	0.75	15.7	20.54	0.25	3.26	23.9	266	238	254	281	292
GeoB1105-4	0.8	16.4	20.13	0.25	2.86	22.4	302	277	287	316	324
GeoB1105-4	0.89	18.0	20.12	0.25	2.66	21.6	295	273	280	310	330
GeoB1105-4	0.95	19.1	20.21	0.25	2.81	22.2	290	261	272	309	334
GeoB1105-4	1.05	20.4	20.22	0.25	*2.75*	*22.0*	284	262	271	300	316
GeoB1105-4	1.15	21.5	19.86	0.25	2.69	21.7	330	301	310	348	367
GeoB1105-4	1.24	23.0	20.16	0.25	2.88	22.5	296	263	282	314	328
GeoB1105-4	1.37	24.8	20.35	0.25	2.94	22.7	281	249	266	295	309
GeoB1105-4	1.47	26.8	20.70	0.25	2.95	22.8	238	218	225	252	269
GeoB1105-4	1.57	28.8	20.14	0.25	2.96	22.8	303	270	286	319	331
GeoB1105-4	1.57	28.8	20.59	0.25	3.01	23.0	254	225	239	269	275
GeoB1105-4	1.67	30.8	20.73	0.25	3.03	23.1	244	218	230	258	268
GeoB1523-1	0.05	3.1	20.78	0.25	4.65	27.8	273	251	259	285	299
GeoB1523-1	0.10	6.0	20.72	0.25	4.47	27.4	277	253	265	294	300
GeoB1523-1	0.15	8.5	20.97	0.25	4.56	27.6	252	234	239	265	279
GeoB1523-1	0.20	10.5	20.73	0.25	4.29	26.9	273	245	258	287	300
GeoB1523-1	0.25	12.6	21.29	0.25	4.14	26.5	217	197	203	228	234
GeoB1523-1	0.30	14.6	21.13	0.25	4.02	26.2	229	210	218	239	258
GeoB1523-1	0.35	16.6	21.33	0.25	3.56	24.9	201	183	191	210	221
GeoB1523-1	0.40	18.2	21.37	0.25	3.68	25.2	203	181	191	214	219
GeoB1523-1	0.45	19.1	21.15	0.25	3.53	24.8	216	197	205	226	234
GeoB1523-1	0.55	20.9	21.14	0.25	3.81	25.6	222	206	212	232	242
GeoB1523-1	0.65	23.9	20.99	0.25	3.69	25.3	235	217	222	246	254
GeoB1523-1	0.75	27.4	21.17	0.25	3.69	25.2	219	200	208	229	240
GeoB1523-1	0.85	30.9	20.67	0.25	3.58	24.9	265	242	249	279	294
ODP 999A	0.05	3.9	20.67	0.25	4.80	28.2	288	268	273	303	310
ODP 999A	0.11	4.6	20.78	0.25	4.91	28.4	278	249	261	295	309
ODP 999A	0.15	5.0	20.59	0.25	4.76	28.1	299	268	283	319	332
ODP 999A	0.31	7.8	20.82	0.25	4.81	28.2	275	249	260	292	300
ODP 999A	0.31	7.8	20.72	0.25	4.81	28.2	279	254	265	294	310
ODP 999A	0.39	9.5	20.68	0.25	4.54	27.6	279	250	263	295	303
ODP 999A	0.43	10.3	20.93	0.25	4.51	27.5	256	230	240	269	282
ODP 999A	0.48	11.7	20.72	0.25	4.33	27.0	271	247	258	283	296
ODP 999A	0.57	14.0	20.98	0.25	4.48	27.4	251	229	237	264	270
ODP 999A	0.61	15.1	21.02	0.25	4.48	27.4	244	224	231	259	268
ODP 999A	0.61	15.1	21.15	0.25	4.48	27.4	233	213	224	242	248
ODP 999A	0.71	17.3	21.04	0.25	4.20	26.7	237	217	224	248	262
ODP 999A	0.82	19.2	21.75	0.25	4.03	26.2	183	168	174	191	200
ODP 999A	0.93	21.1	21.20	0.25	3.90	25.9	220	206	209	230	240
ODP 999A	1.02	22.5	21.26	0.25	4.21	26.7	220	203	207	231	239
ODP 999A	1.13	24.8	21.51	0.25	4.09	26.4	199	182	192	208	223
ODP 999A	1.20	26.3	21.62	0.25	4.04	26.3	191	173	181	201	209
ODP 999A	1.20	26.3	21.69	0.25	4.04	26.3	185	170	175	195	205

pCO_2^{sw} calculated as described in text and assuming a constant total alkalinity of 2300 mmol/kg. Uncertainty determined using a Monte Carlo approach (n=10,000). 95 % of Monte Carlo simulations lie between 2.5 and 97.5 percentiles, 68% lie between 14 and 86 percentile Mg/Ca and boron isotope data for ODP 999A and GeoB1523-1 have been published in Foster (2008) and Henehan et al. (2013), respectively but are recalculated here for consistency. pCO_2^{sw} differences between the data here and the previously published records is minor (on average ~6 matm).

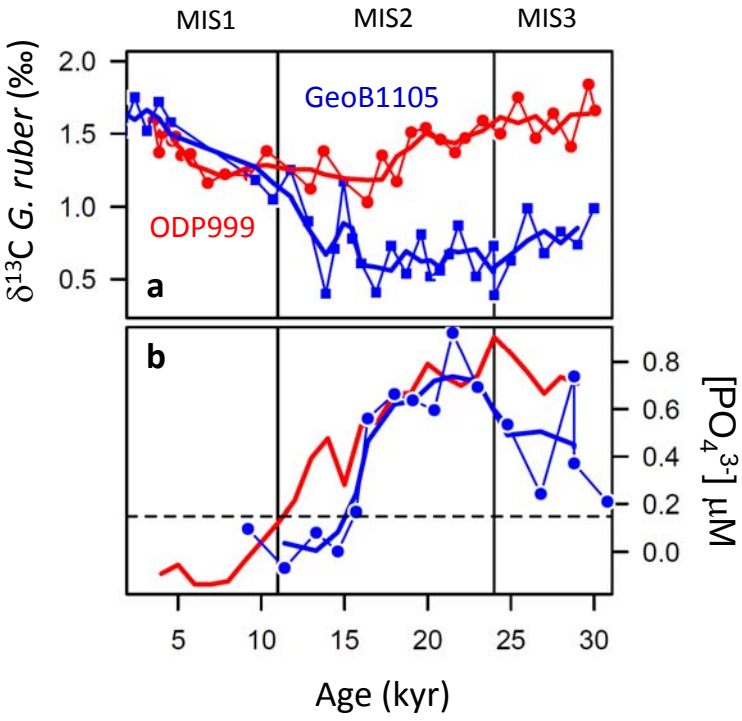

Figure DR1. Foster & Sexton

(a) G. ruber $\delta^{13}C$ (‰) from Schmidt et al., (2004) and Mulitza et al. (1998) for sites ODP 999 (red) and GeoB1105 (blue). (b) Phosphate concentration (in µM) at GeoB1105 calculated from the $\delta^{13}C$ gradient (red) and the excess-DIC from boron isotope based estimates of ΔpCO_2 (blue). The dotted line in (b) shows the modern phosphate concentration at GeoB1105. Vertical lines denote the boundaries of marine isotope stages (MIS).